ASTRONOMY & ASTROPHYSICS
SUPPLEMENT SERIES

Astron. Astrophys. Suppl. Ser. **39**, 215-233 (1980)

WESTERBORK SYNTHESIS OBSERVATIONS OF 8 CLUSTERS OF GALAXIES WHICH CONTAIN TAILED RADIO GALAXIES

D. E. HARRIS ([1, 3]), V. K. KAPAHI ([1]) (*) and R. D. EKERS ([2])

([1]) Netherlands Foundation for Radio Astronomy, Dwingeloo, the Netherlands
([2]) Kapteyn Laboratory, University of Groningen, Postbus 800, Groningen, the Netherlands
([3]) Dominion Radio Astrophysical Observatory, Box 248, Penticton, B.C. V2A 6K3 Canada

Received March 19, 1979

Summary. — Observations of A401, A1446, A1452, A1775, A2220, A2250, A2255, and A2306 are presented at 1 415 MHz with supplementary observations at 610 or 4 995 MHz for most of the clusters. Positions, intensities, and optical identifications are tabulated for all the sources found in the 8 fields, and contour diagrams are given for sources of complex brightness distribution.

We discuss the nature of the low-frequency (< 100 MHz) emission for 3 clusters on the basis of our spectral data. As an alternative to the usual model of radio halos residing in the core of clusters, we suggest that non-thermal (and perhaps thermal) emission may arise at an interface between subclusters which are in the process of coalescing.

Key words : Tailed radio galaxies — Clusters of galaxies.

1. **Introduction.** — The present paper represents partial results of a program to map tailed radio galaxies with the good sensitivity for low surface brightness afforded by the Westerbork Synthesis Radio Telescope (WSRT). The clusters A401 and A2255 were selected from the sources originally observed at Cambridge by Slingo (1974). A1446, A1452, A1775, A2220, and A2250 were brought to our attention by Owen after his initial observations at the National Radio Astronomy Observatory. The complex source in A2306 was found by de Bruyn during the course of observations of NGC 6643, a nearby spiral galaxy.

Section II gives a brief description of the observations and reduction procedures ; section III contains remarks on each cluster ; and section IV discusses some of the problems associated with radio halos and the interaction of binary clusters.

2. **Observations and reductions.** — The WSRT system has been described in detail by Baars and Hooghoudt (1974), Högbom and Brouw (1974), and Weiler (1973). The parameters relevant to the present observations are given in table I.

After the *u-v* data were transformed into brightness maps, cleaning and measuring of source parameters were performed at the University of Groningen with the interactive programs described by Ekers *et al.* (1973). We used 4 methods to obtain estimates of the source parameters. (1) Fitting the synthesized beam shape to a source produced the coordinates, α, δ, and the flux density, S, for unresolved sources. (2) Fitting a two-dimensional Gaussian produced α, δ, S, and size parameters (half-power diameters and position angles of the major and minor axes) for moderately resolved sources. (3) Cleaning the source (Högbom, 1974) produced S as the sum of the components. (4) Integration of the map over a box enclosing extended sources produced another estimate of the total flux density. All determinations of S were corrected for the primary beam attenuation.

Optical identifications for each radio source were sought by the overlay procedure and then by measuring positions of optical objects on the PSS (Palomar Sky Survey) *E* prints to an accuracy of about one arcs with the measuring machine of the Sterrewacht in Leiden.

3. **Results.** — *a*) DESCRIPTION OF THE SOURCE LISTS. — Tables II-VIII and X are source lists for the 8 fields in order of increasing right ascension. The assigned serial numbers, when preceded by the code number « 14 W », serve to identify each source. Columns 2 and 3 list 1950 coordinates (from the 1 415 MHz observations) and formal 1 σ errors generated by the 2-dimensional Gaussian fitting procedure (with a minimum value of approximately one arcs, the systematic uncertainty). The 2 σ errors for the listed flux densities were estimated from fitting errors, estimates of the uncertainty in the level of the map around the source, and from a comparison of the various methods used to measure the flux density. A further systematic error of $\pm$ 5 % arises from the uncertainty of the flux density scale. For tables II (A401) and VIII (A2255) the spectral index α (defined by $S_\nu = A\nu^{-\alpha}$) has been calculated from the flux densities measured at 610 and 1 415 MHz. Although no search routines were used in the reductions, a completeness level of 10 mJy (no correction for primary beam attenuation) may be assigned to all of the 1 415 MHz maps except that of A2306 where a few sources in the 10-20 mJy range *could* have been missed.

(*) Present Address : Tata Institute of Fundamental Research, Bombay 400005, India.

Information about the optical field and the suggested identification is given in the next to last column. The abbreviations used for type of object are :

PLO : Plate limit object.
G : Galaxy.
S : Stellar image.
EF : Empty field (no optical objects within 10″).

A single asterisk before the optical type means that the difference between the optical and radio position lies between 2 and 5 times the listed error in the radio position, σ. A double asterisk indicates that the positions agree to within 2 σ. A question mark following the optical type means that the classification given is uncertain. An estimate of the visual magnitude is given in parenthesis for galaxies brighter than 18 m. Otherwise an « f » for *faint* or a « b » for stars judged to be brighter than 18 m is given. A dagger following the magnitude estimate indicates that the galaxy could well be a member of the cluster (positioned within one Abell radius of the cluster center and having a brightness within two magnitudes of m_{10}, the magnitude of the tenth brightest member).

For those sources for which the optical object was measured to an accuracy of one arcs, the position differences in right ascension ($\Delta\alpha''$) and declination ($\Delta\delta''$) are listed in the sense radio position minus optical position.

The *Notes* column contains three kinds of information. (1) When a source was significantly resolved, the results of the two-dimensional Gaussian fitting procedure at 1 415 MHz are given. These are the deconvolved half-power diameters in arcs followed by the position angle, *PA*, of the major axis in degrees. (2) For sources which have been previously catalogued (October 1973 version of Dixon's *Master List of Radio Sources :* see section V of Dixon, 1970) a « 4C », « B2 », « Ohio », or « VRO » is listed. (3) Letters indicate that more extensive notes are given following the table.

b) A401 (DISTANCE CLASS D = 3, RICHNESS CLASS R = 2, m_{10} = 15.6). — Hintzen *et al.* (1977) have measured the redshifts of 14 galaxies in this field and find z = 0.0746 (D = 448 Mpc) ([1]), and the velocity dispersion $\sigma = 1\,390\ \sqrt{3}$ km s^{-1}. X-ray emission from this field has been observed by many satellites ; the more recent articles are by Ulmer *et al.* (1979), Maccagni *et al.* (1978), Forman *et al.* (1978), and Cooke *et al.* (1978). The emission appears to be extended (diameter estimates range from 12′ to 50′) and centered somewhere near $\alpha = 02^h56^m$, $\delta = 13°12'$ (i.e. about halfway between A401 and A399, a companion cluster (D = 3, R = 1, m_{10} = 15.6). J. Hutchings of the Dominion Astrophysical Observatory has kindly determined the radial velocity of the bright galaxy at the center of A399. He reports z = 0.071, i.e. confirming that A399 is at the same distance as A401. HEAO-2 observations should determine whether both clusters are X-ray sources or whether the emission is actually centered between the clusters.

Our data at 1 415 MHz have been supplemented with 610 MHz data taken from an early WSRT map kindly supplied by G. K. Miley (see Table II). A map of the tailed radio galaxy (TRG) at 1 415 MHz is shown in figure 1. Hintzen *et al.* (1977) have argued that acceleration is necessary in the tail because the tail is so long (7′) that the electrons at the end of the tail would otherwise be many times older than their halflife. Because our resolution is poor in declination, it is difficult to determine the projected length of the tail. Our best estimate comes from the effective beam deconvolution which occurs during cleaning. The southernmost components are at $\delta = 13°18'$ (3 σ, 1 415 MHz), and at $\delta = 13°16'.7$ (2.7 σ, 610 MHz : length = 5′.9). These values do not change the conclusions reached by Hintzen *et al.*

Several other sources in the field are identified with galaxies which are probable members of A401 (lying within 3 Mpc of the cluster center and brighter than m_{10} + 2). Source *12,* near the edge of the cluster is a bent double (see Fig. 2). 4C13.17B (*21*), is extended and is probably associated with one or both of two close galaxies (the brighter is No. 4 of Hintzen *et al.,* 1977, and is a member of the cluster). *14* is unresolved and *1* may be associated with Abell 399.

Source *24* (4C13.17C) is occasionally thought to be associated with A401 (e.g. Ulmer *et al.,* 1979). Slingo (1974) gives a finding chart and indicates the positions of two faint objects on his contour diagram. Figure 3 is a reproduction of a 13 minute (red) exposure with the 4m telescope of the Kitt Peak National Observatory (ISIT Vidicon TV camera). We believe that *24* is a background source for the following reasons :

a) Slingo's two objects are stellar and neither lies at the radio centroid.

b) The faint filament visible on the PSS E print just to the north of Slingo's western object is a plate defect.

c) There is a faint galaxy with m_r = 21.0 at $\alpha = 02^h56^m53^s.08$, $\delta = 13°43'04''.1$: i.e. within 0.5 arcs of the radio centroid. This appears to be the correct identification. For q_0 = 0.5 and $M_v \sim -22.5$, the overall radio size would be $\lesssim$ 300 kpc, and the radio luminosity would be somewhat less than that of Cyg A.

The structure and optical identification of *19* are relevant to the discussion of the low frequency emission from the cluster (see section IV). Figures 4*a* and 4*b* show the area around *19* at 1 415 MHz and 610 MHz. While no bright galaxies coincide with the peak of the source, several lie close by. The cross at the bottom of the figures shows the position of the central cD galaxy (No. 2 of Hintzen *et al.*). The flux densities listed in table II have been derived from a map integration over the whole source. The resulting spectrum is steep (α = 1.3 ± 0.3) and this source could represent the brighter parts of a halo source. Until high resolution maps at low frequencies become available it is difficult to be sure that the emission surrounding *19* is actually associated with the cluster, but if it is a background source, it would have to be larger than 400 kpc.

c) A1446 (D = 5, R = 2, m_{10} = 17.0). — No redshift is available for this cluster but Owen and Rudnick (1976) give an estimated value of 0.131. Figures 5*a* and 5*b* show contour diagrams of the bent double at the

([1]) Throughout this paper we have taken H_0 = 50 km s^{-1} Mpc^{-1}.

cluster center, 4C58.23 (*33* in Table III). Compared to the 2 695 MHz maps of McHardy (1978) and of Owen and Rudnick (1976), no new features are observed. The spectrum from 22 to 8 085 MHz is defined by a power law with $\alpha = 0.9$.

The galaxy identified with this source is much brighter than others in the cluster and a double nucleus is visible on the PSS O print. Spectroscopic observations of both components as well as several other cluster galaxies are needed to determine if the central galaxy has a low velocity with respect to the cluster mean (see the discussion in Owen and Rudnick, 1976).

None of the other sources in table III appear to be associated with the cluster although *35,* identified with an 18^m6 galaxy, could be an outlying member.

d) A1452 ($D = 4$, $R = 0$, $m_{10} = 15.7$). — The central source (4CP51.29a) in this cluster has been observed by Rudnick and Owen (1976, 1977) with the NRAO interferometer and velocities of 15 cluster members have been determined by Ulrich (1978). The redshift is $z = 0.0627$, distance = 376 Mpc, and velocity dispersion, $\sigma = 503\sqrt{3}$ km s^{-1}. WSRT observations at 1 415 MHz of the central source (*44*) are given in Miley and Harris (1977). In this paper we give the parameters for all the sources measured in the field at 1 415 MHz (Table IV) and the 4 995 MHz map of the central source.

In addition to *44,* there are two sources (*43* and *46*) identified with bright galaxies. *46* has been shown to belong to a group of galaxies at $z \sim 0.083$ (Ulrich, 1978) and *43* is only 23″ from another member of this background group.

Figure 6 is a contour diagram of *44* at 4 995 MHz where the brighter parts of the western component can be seen. Flux densities of both components were derived by integrating the same areas used for the 1 415 MHz integration : the eastern component = 179 mJy and the western component = 51 mJy (± 10 % for each). The spectral indices are α (east) = 0.7 ± 0.1, and α (west) = 1.0 ± 0.15. Although a point-by-point spectral index calculation has not been made, it is unlikely that there are large departures from a uniform spectral index distribution within each component. The 4 995 MHz map, when smoothed to the resolution of the 1 415 MHz map, reproduces all the features above the second contour level of the 1 415 MHz map of Miley and Harris (1977).

Ulrich (1978) has shown that the radial velocity of the galaxy associated with *44* is only 200 km s^{-1} with respect to the cluster average. Therefore, either the space velocity is rather small (< 300 km s^{-1}) or else the transverse velocity is greater than the radial velocity. In either case it would be unwarranted to assume large projection effects when attempting to explain the complex radio morphology.

If a *wide angle tail* model is suggested in order to account for the western component, then the galaxy must now be ejecting in one direction only.

It would be useful to obtain an optical spectrum of the faint galaxy at $\alpha = 12^h00^m28^s0$, $\delta = 51°56'43''$ to determine if it is associated with the cluster. Although no radio emission has been detected from this galaxy, it lies close to the extrapolated arc which traces the brightness ridge of the western component.

e) A1775 ($D = 4$, $R = 2$, $m_{10} = 15.7$.) — The TRG in this cluster has been discussed by Slingo (1974), Owen *et al.* (1977), and Miley and Harris (1977). Here we include 1 415 MHz data on other sources in the field (Table V), and results of WSRT observations at 4 995 MHz.

Hintzen (1979) has measured the radial velocities of nine galaxies in A1775. Although he finds a bimodal distribution of velocities, he favors a one-cluster interpretation with $< v > = 20{,}859$ km s^{-1}, ($z = 0.0695$, $D = 417$ Mpc) and $\sigma = 1\,522\sqrt{3}$ km s^{-1}.

Figure 7 shows that the north-west member of VV5-32-63/64 is probably a weak radio source, in agreement with the NRAO results at 2 695 MHz (Owen *et al.* 1977). The flux density of that part of the TRG (*55* in Table V) visible in the figure is 80 mJy (4 995 MHz).

The overall spectrum of 4C26.41 (the TRG) is well represented by a power law with $\alpha = 1.0$ between 400 and 8 000 MHz. Below 100 MHz, however, the spectrum steepens to $\alpha = 1.6$ (Viner and Erickson, 1975, Roger, private communication : S (22 MHz) = 89 Jy). At 1 415 MHz, the head of the TRG is well defined and is much brighter than the tail. Thus we may separate the flux density at this frequency into two components : 240 mJy in the head and 120 mJy in the tail. If we then suppose that the excess low frequency emission comes from the tail, power law spectra may be constructed with α (tail) = 1.5 and α (head) = 0.9.

Two other sources in table V have been identified with galaxies. The brighter of these (*51*, a 15.9 m galaxy) is number 208 of Hintzen (1979) and is a cluster member.

f) A2220 ($D = 6$, $R = 0$, $m_{10} = 17.5$). — The central source 4C53.37 (*74* in Table VI) appears to be a *bent double* (see Fig. 8*a* and 8*b*). Source parameters at 2 695 and 8 085 MHz are given by Rudnick and Owen (1977), and McHardy (1978) gives the results of Cambridge observations at 408, 1 407, and 2 700 MHz.

The redshift of the bright galaxy identified with *74* has been measured by Ulrich (1976) to be $z = 0.1098$ ($D = 660$ Mpc). This corresponds to $m_{10} = 16.7$, distance class 5. More velocity measurements are needed to confirm that 0.1098 is the systemic redshift for the cluster, i.e. that Abell's estimate of the distance class is wrong rather than the possibility that *74* has a large peculiar velocity with respect to the cluster mean.

Two other sources listed in table VI which are identified with galaxies could be cluster members. *76* is unresolved and lies at a projected distance of 2.3 Mpc from the cluster center. *79,* identified with a 16 m galaxy, lies at a projected distance of 4.3 Mpc from the cluster center. Figure 9 shows the weak wings which extend 1′.5 (~ 290 kpc) to the east and west of the unresolved central component.

g) A2250 ($D = 5$, $R = 1$, $m_{10} = 16.5$). — As for A2220, the distance to this cluster is much closer than that estimated from m_{10}. Ulrich (1978) gives $z = 0.0653$ ($D = 392$ Mpc), and $\sigma = 693\sqrt{3}$ km s^{-1}.

The TRG in this cluster (*90* in Table VII) has been discussed by Rudnick and Owen (1976, 1977) and by Miley and Harris (1977). Our radio map at 4 995 MHz is shown in figure 10. No sign of a double structure is seen and the tail can be traced for only 0.′5, compared with 6.′0 (687 kpc) for the distance from the galaxy to the last component (5 σ) at 1 415 MHz. The radial velocity of the galaxy is 760 km s^{-1} with respect to the cluster mean (Ulrich, 1978).

The only other source in table VII which is identified with a galaxy is *89*. Since this galaxy is so faint ($m_v \sim 18.5$), a velocity determination is necessary before cluster membership can be assumed.

h) A2255 ($D = 3$, $R = 2$, $m_{10} = 15.3$). — Tarenghi and Scott (1976) have measured radial velocities for several galaxies in this cluster and suggest that there are actually two clusters superimposed with a velocity difference of 2 500 km s^{-1}. For purposes of scale size and luminosity estimates, we adopt a mean distance of 473 Mpc ($z = 0.0788$).

Cooke and Maccagni (1976) have reported a 4.3 σ X-ray detection from this cluster with $L_x = 7 \times 10^{44}$ ergs s^{-1}. However, Ricketts (1978) reports an upper limit of 0.4 Ariel V c/s ($L_x < 4 \times 10^{44}$ ergs s^{-1}).

Aperture synthesis observations of A2255 have been made at 408 and 1 407 MHz by Slingo (1974) and at 2 695 and 8 085 MHz by Rudnick and Owen (1976, 1977). Slingo discussed four sources associated with the cluster : 4C64.20.1A, B, C, and a weak source « S » detected at 408 MHz but not at 1 407 MHz. At the position of « S » we find no indication of an unresolved source : S (1 415 MHz) < 1 mJy, S (610 MHz) < 12 mJy. The nearby bright galaxy however, is a weak source : S (1 415 MHz) = 2.1 mJy, our source *117*. Slingo suggested that « S » was unresolved and responsible for the low-frequency emission ($\alpha \sim 2.6$). If this were the case, we should have detected it at about 4 mJy (1 415 MHz), and at about 40 mJy (610 MHz).

Although centimetre wave observations do not allow us to determine the location of the excess emission at metre wavelengths, a strong case can be made that the steep spectrum component of the total emission which is observed below 100 MHz originates in a halo. Spectra of the discrete sources in the field are known (Table VIII), and if these spectra are *extrapolated* to lower frequencies, the sum of the flux densities (e.g. S_{22} (*115, 118, 120*) $\approx$ 20 Jy) cannot account for the total emission below 100 MHz ($S_{22} = 83 \pm 12$ Jy ; Roger, private communication). Direct evidence of halo emission is provided by our 610 MHz map (Fig. 11*b*) and from the 1 415 MHz map when it is smoothed to lower resolution. Jaffe and Rudnick (1979) give further evidence for halo emission from A2255.

A map integration at 610 MHz for the entire area shown in figure 11*a* yields a value of 1.45 Jy. If the flux densities of *115, 116, 118,* and *120* are subtracted from this figure, we obtain a halo flux density of 0.20 Jy at 610 MHz. 60 % of this lies to the north of the TRG. The spectral index of the halo would then be 1.7. These estimates are meant to be indicative only, since it is impossible to make a clear distinction between the tail and the halo.

One could, for example, maintain that the emission to the north of the TRG should be considered as a proper part of the tail. If one traces the *ridge line* of the contour diagram away from the galaxy, it first rotates counterclockwise 50° (Fig. 11*a*) and then clockwise 110° (Fig. 11*b*). At least in this case the rather sharp bends in the projected tail could be interpreted in terms of the trajectory of the TRG : bright galaxies are found in the locations required to produce the observed deflections. Whichever way one divides the emission between tail and halo, our maps are consistent with the hypothesis that radio halos represent relics of tails (Harris and Miley, 1978).

Unlike the other clusters studied in this paper, A2255 contains many radio galaxies. To make the following discussion more readable, we have adopted descriptive names for the extended sources (Table IX).

i) 4C64.20.1 A. THE ORIGINAL TRG (*115*). — We find that the radio peak is polarized at about 1.4 % in $PA = 45°$. Figure 11*a* shows a contour diagram at 1 415 MHz which is essentially the same as Slingo's map. Note however, the appearance of a weak source (*113*) which is probably associated with a cluster galaxy to the west of the TRG.

ii) 4C64.20.1 B. THE GOLDFISH (*118*). — This source is shown in figures 11*a* and 11*b*. The tail is quite weak and extends about 290 kpc to the south. The polarization of the head is ≤ 4 %. The velocity of the galaxy is close to the mean value of cluster B (Tarenghi and Scott, 1976).

iii) 4C64.20.1 C. THE DOUBLE (*120*). — Rudnick and Owen (1977) have shown that this source is a triple with the outer components separated by 25″ (58 kpc) in $PA = 10°$. The northeast lobe appears to be polarized at 1 415 MHz, ~ 1.3 % in $PA = 35°$. No polarization above the noise level was detected from the southwest lobe ($P < 1$ %).

iv) THE BEAVER (*119*). — This source extends over 400 kpc at 610 MHz and is shown in figures 12 (*a* and *b*). At 1 415 MHz there are two patches of polarized emission : 10″ west of the northern radio peak we find 12 %, $PA = 170°$ and about 10″ northwest of the southern radio peak we find 12 % in $PA = 90°$.

Although the general morphology of the *Beaver* is that of a TRG, there are 3 peculiarities. (1) Unlike most TRGs which lie at a projectal distance of < 1 Mpc from their cluster centers, the *Beaver* is ≥ 2.6 Mpc from the center of A2255. (2) The spectrum is rather flat. Although our data do not allow an accurate determination of the spectral index ($\alpha = 0.5 \pm 0.3$), the flux density at 2 695 MHz (Haslam *et al.* 1978) is reported to be 166 mJy (i.e. larger than our 1 415 MHz integrated value). (3) Whereas the radio centroid is usually closer to the parent galaxy for higher frequencies (reflecting the general steepening of the spectrum down the tail), the Bonn position is only 0.′1 from our 610 MHz centroid (just south of the northern peak in figure 12*a*). Furthermore, unlike most TRGs, the peak brightness occurs halfway down the tail rather than close to the galaxy. Redshifts for the two galaxies shown in figure 12 as well as high resolution radio observations at 5 000

MHz are necessary to determine the nature of the *Beaver.*

v) THE EMBRYO (*127*). — This source appears to be a *bent double,* as can be seen in figures 13*a* and 13*b*. Close to the nothernmost galaxy ($\delta \sim 64°06'$) we find 16 % polarization with a $PA = 90°$ at 1 415 MHz. Just to the north, in the plateau between the center peak and the northern peak, ($\delta \sim 64°07'$), the percentage polarization is about the same, ~ 15 %, $PA = 25°$. In the southern lobe the polarization is a bit smaller : 9 %, $PA = 170°$.

For the optical identification, we favor the bright galaxy coincident with the peak radio intensity. The cross between the central component and the southern component indicates the position of a much fainter galaxy which is elongated.

Since the *Embryo* lies at a projected distance of 2.5 Mpc from the cluster center, radial velocity data are needed to confirm cluster association.

vi) THE BEAN (*128*). — Even though this source lies at a projected distance of 5.3 Mpc from the center of A2255 there is good evidence to support cluster membership. The *Bean* is resolved (Fig. 14) and tentatively may be classified as a bent double. The optical identification is a 16 magnitude elliptical galaxy, almost identical in appearance to that associated with the *Embryo*. Furthermore, the *Bean* is well within Zwicky's boundary of the cluster.

vii) In addition to the above, table IX lists four weaker sources which are associated with galaxies within 3 Mpc of the cluster center and brighter than ($m_{10} + 2$). Redshift determinations are needed for three of these. By any standards, A2255 is a remarkable cluster and we urge optical astronomers to obtain many more velocities : not only for the galaxies which are associated with radio sources, but also for enough galaxies to evaluate the two-cluster hypothesis proposed by Tarenghi and Scott. The corresponding Zwicky cluster, *Z*w 1 710.4 + 6 401, has a N-S extent of 16 Mpc.

viii) A2306 ($D = 5, R = 0, m_{10} = 17.0$). — The sources near the cluster center (*135, 136* and *137*) were found by G. de Bruyn on a WSRT map of NGC6643. They have also been mapped at 2 695 MHz by Rudnick and Owen (1977) who have shown that *135,* the northwest companion of the wide angle tail, is a close double with a separation of 13″ in $PA = 124°$.

To the best of our knowledge, no redshift is available for A2306 and we assume $z = 0.125$, based on $m_{10} = 17.0$. The source at the cluster center (*136*) bears a striking resemblance to 3C66B (compare figure 15 with the WSRT map by Miley and van der Laan, 1973). If A2306 is at $z = .125$ ($D = 750$ Mpc) it is ~ 7 times less luminous but twice as large as 3C66B. If, however, z (A2306) were to be 0.25 (i.e. at the same distance as 3C379.1, identified with an 18 *m* galaxy, 22′ to the south of A2306), then it would be about half the luminosity of, but over 4 times larger than 3C66B.

Polarization measurements are hampered by instrumental effects of 3C379.1. However, the radio peaks of both *136,* the wide angle tail, and *135,* the close double, are about 5 % polarized. The position angles of the electric vectors are $\sim 90°$ and $\sim 100°$, respectively.

No optical identification for the close double has been found so we cannot assume it is associated with the cluster (compare with the situation in A2255). However, the extended source, *137,* just to the northeast of the wide angle tail may be associated with the cluster since there are two galaxies close to the peak.

Other radio galaxies which qualify for cluster association are *140* and *142* ; both are within the Abell radius and brighter than ($m_{10} + 2$).

4. **Discussion.** — Because of the difficulty of obtaining brightness distributions below 100 MHz with resolutions of one arcmin, two hypotheses have been advanced as to the spatial nature of the low-frequency emission which is often found to be associated with clusters of galaxies. Slingo (1974), Guthrie (1977), and others have argued that the intergalactic gas inferred from thermal bremsstrahlung models of X-ray emission confines discrete sources for a time which is sufficient to allow E^2 losses to steepen their spectra. Willson (1970) and others have taken the view that the low frequency emission is well distributed in the sense that is would not be possible to associate it with a particular galaxy, i.e. halo emission.

Three of the clusters discussed in this paper have steep spectra below 100 MHz. For A2255 (section III*h*), we find no evidence of a *confined* source with a spectrum which could explain the low frequency emission. The halo interpretation on the other hand, is supported by our 610 MHz maps (Fig. 11*b*).

Although no halo has been detected in A1775 (observations at 610 MHz to search for a halo were not undertaken because we anticipated dynamic-range problems), the 26 MHz position (Viner and Erickson, 1975) is just to the east of the tail.

The situation in A401 is more complex. From spectral data alone, we could associate *19* with the low frequency data of Braude *et al.* (1978), Williams *et al.* (1966), and Viner and Erickson (1975) : $\alpha = 1.6$. However *19* lies to the northeast of the cluster center while all the low frequency positions are 0°.3 to 0°.5 to the south of the cluster center. None of our sources in this southern area has a spectrum which could be extrapolated to include the low frequency data. In the absence of a halo component at 610 MHz, the best evidence for the distributed nature of the low-frequency emission comes from an estimate of the source diameter of 30′ at 22 MHz (Costain, private communication of beam broadening).

It has been suggested (e.g. Harris and Miley, 1978) that radio halos may be relics of TRGs. This hypothesis is supported by our data for A2255 (Fig. 11*b*), and by the best available positions of the low-frequency emission from Abell 401 and 1775. Taken at face value, the observational data for A401 indicate non-thermal emission from a region between A399 and A401. One could imagine an interface between two subclusters undergoing coalescence (see White, 1976). Particle acceleration by the Fermi mechanism would be expected under these conditions : a collision of two gas clouds together with

their associated fields could reaccelerate relativistic electrons from the relic tail.

We must then ask why the X-ray emission appears to be centered on the same area (see section III*b*). On the conventional thermal bremsstrahlung model for X-ray emission from clusters, it would seem necessary that the hot gas should occur in the potential wells delineated by the galaxy distributions.

A thermal origin for the X-rays could be explained by a density and/or temperature enhancement at the interface. In this case we would expect that the X-ray brightness distribution could display three maxima : at the cluster centers and at the interface. Alternatively, at X-ray frequencies for which non-thermal emission dominates, the X-ray distribution should mimic the low-frequency distribution (presumably single-peaked). Although HEAO-2 observations should delineate the soft X-ray distribution, low-frequency ratio data with sufficient resolution are not likely to be available in the near future.

A1775 (Hintzen, 1979) and A2255 (Tarenghi and Scott, 1976) may represent other examples of binary clusters undergoing coalescence. Both cases should be checked by observations of many more galaxies. For example, one may ask why the double radio galaxy (*120*) in A2255 is not a TRG. On the two-cluster model, the radial velocity of the TRG is 412 km s^{-1} with respect to the mean of cluster B, whereas this figure is 650 km s^{-1} for the double. On the one-cluster model, however, the double has the same radial velocity as the cluster mean and no distortion of the radio structure is expected.

It is remarkable to find evidence of intracluster gas from radio galaxies of deformed morphologies at large distances from the nominal center of A2255. Even if the *Bean* (5.3 Mpc from the cluster center) is not associated with the cluster, both the *Embryo* and the *Beaver* are at a projected distance of 2.5 Mpc. In view of the presence of many deformed radio galaxies and the possible double nature of A2255, it seems likely that this cluster will be detected by HEAO observations. However, it is doubtful that X-ray observations will provide the kind of evidence available for A401 on the possibility of an interface between the subclusters. The TRG, the radio halo, and the giant galaxies of both clusters, all lie close to the same line of sight.

Acknowledgements. — It is a pleasure to thank J. Hutchings for determining the redshift of the bright galaxy in A399 and H. Butcher for his patient instruction on the operation of the ISIT VIDICON and for the reduction of the 4m data. We also acknowledge the assistance of G. K. Miley and R. G. Strom in early stages of data reduction. M. H. Ulrich kindly sent us useful data prior to publication and the D.R.A.O. staff suggested many improvements in the text.

The Kitt Peak National Observatory is operated by the Association of Universities for Research in Astronomy, Inc., under contract with the National Science Foundation. The Westerbork Synthesis Radio Telescope is operated by the Netherlands Foundation for Radio Astronomy with financial support from the Netherlands Organization for the Advancement of Pure Research (Z.W.O.).

References

Baars, J. W. M., Hooghoudt, B. G. : 1974, *Astron. Astrophy.* **31,** 323.
Braude, S. Ya., Megn, A. V., Rashkovski, S. L., Ryabov, B. P., Sharykin, N. K., Sokolov, K. P., Tkatchenko, A. P., Zhouck, I. N. : 1978, *Astrophys. Space Sci.* **54,** 37.
Cooke, B. A., Maccagni, D. : 1976, *Mon. Not. R. Astron. Soc.* **175,** 65p.
Cooke, B. A., Ricketts, M. J., Maccacaro, T., Pye, J. P., Elvis, M., Watson, M. G., Griffiths, R. E., Pounds, K. A., McHardy, I., Maccagni, D., Seward, F. D., Page, C. D., Turner, M. J. L. : 1978, *Mon. Not. R. Astron. Soc.* **182,** 489.
Dixon, R. S. : 1970, *Astrophys. J. Suppl.* **20,** 1.
Ekers, R. D., Allen, R. J., Luyten, J. R. : 1973, *Astron. Astrophys.* **27,** 77.
Forman, W., Jones, C., Murray, S., Giacconi, R. : 1978, *Astrophys. J.* **225,** L1.
Guthrie, B. N. G. : 1977, *Astrophys. Space Sci.* **52,** 177.
Harris, D. E. and Miley, G. K. : 1978, *Astron. Astrophys. Suppl.* **34,** 117.
Haslam, C. G. T., Kronberg, P. P., Waldthausen, H., Wielebinski, R., Schallwich, D. : 1978, *Astron. Astrophys. Suppl.* **31,** 99.
Hintzen, P., Scott, J. S., Tarenghi, M. : 1977, *Astrophys. J.* **212,** 8.
Hintzen, P. : 1979, preprint.
Högbom, J. A., Carlsson, I. : 1974, *Astron. Astrophys.* **34,** 341.
Högbom, J. A., Brouw, W. N. : 1974, *Astron. Astrophys.* **33,** 289.
Högbom, J. A. : 1974, *Astron. Astrophys. Suppl.* **15,** 417.
Jaffe, W. J., Rudnick, L. : 1979, *Astrophys. J.* (in press).
Maccagni, D., Tarenghi, M., Cooke, B. A., Maccacaro, T., Pye, J. P., Ricketts, M. J., Chincarini, G. : 1978, *Astron. Astrophys.* **62,** 127.
McHardy, I. M. : 1978, *Mon. Not. R. Astron. Soc.* **185,** 927.
Miley, G. K., van der Laan, H. : 1973, *Astron. Astrophys.* **28,** 359.
Miley, G. K., Harris, D. E. : 1977, *Astron. Astrophys.* **61,** L23.
Owen, F. N., Rudnick, L. : 1976, *Astrophys. J.* **205,** L1.
Owen, F. N., Rudnick, L., Peterson, B. M. : 1977, *Astron. J.* **82,** 677.
Ricketts, M. J. : 1978, *Mon. Not. R. Astron. Soc.* **183,** 51p.
Rudnick, L., Owen, F. N. : 1976, *Astrophys. J.* **203,** L207.
Rudnick, L., Owen, F. N. : 1977, *Astron. J.* **82,** 1.
Slingo, A. : 1974, *Mon. Not. R. Astron. Soc.* **168,** 307.
Smith, H. E., Spinrad, H., Smith, E. O. : 1976, *Pub. Astron. Soc. Pac.* **88,** 621.
Tarenghi, M., Scott, J. S. : 1976, *Astrophys. J.* **207,** L9.
Ulmer, M. P., Kinzer, R., Cruddace, R. G., Wood, K., Evans, W., Byram, E. T., Chubb, T. A., Friedman, H. : 1979, *Astrophys. J.* **227,** L73.
Ulrich, M. H. : 1976, *Astrophys. J.* **206,** 364.

ULRICH, M. H. : 1978, *Astrophys. J.* **221**, 422.
VINER, M. R., ERICKSON, W. C. : 1975, *Astron. J.* **80**, 931.
WEILER, K. W. : 1973, *Astron. Astrophys.* **26**, 403.
WHITE, S. D. M. : 1976, *Mon. Not. R. Astron. Soc.* **177**, 717.
WILLIAMS, P. J. S., KENDERDINE, S., BALDWIN, J. E. : 1966, *Mem. R. Astron. Soc.* **70**, 53.
WILLSON, M. A. G. : 1970, *Mon. Not. R. Astron. Soc.* **151**, 1.

TABLE I. — *Parameters of the observations.*

CLUSTER	FREQUENCY (MHz)	FIELD CENTERS (1950) α	δ	RESTORING BEAM SIZE α	δ	SHORTEST SPACING (metres)	INCREMENT (metres)	RMS NOISE (mJy)	OBSERVATION DATE (Year)
A401	610	$02^h56^m00^s$	13°23′	58.″5	254.″	36	72	3.75	73.8
	1415	02 55 48	13 18	25.1	108.1	[a]	[a]	0.43	75.5
A1446	1415	11 59 31	58 18 45″	25.4	29.9	36	72	0.65	75.6
	4995	11 59 31	58 18 45	7.2	8.5	36	72	1.02	77.1
A1452	1415	12 00 35	51 57	25.4	32.5	36	72	0.60	75.6
	4995	12 00 35	51 57	7.0	8.9	36	18	0.60	76.8
A1775	1415	13 39 31	26 37 30	24.8	55.5	72	72	0.50	75.6
	4995	13 39 31	26 37 30	7.1	16.0	54	72	1.1	77.1
A2220	1415	16 38 25	53 52 30	25.4	31.5	36	72	0.50	75.6
	4995	16 38 25	53 52 30	7.2	8.9	36	72	1.0	77.1
A2250	1415	17 09 17	39 46 10	25.4	39.8	36	72	0.45	75.6
	4995	17 09 17	39 46 10	7.0	11.0	36	18	0.60	76.9
A2255	610	17 12 30	64 06	58.2	64.5	36	72	1.58	77.1
	1415	17 12 30	64 06	25.1	27.9	36	36	0.34	75.5
A2306	1415	18 26 10	74 42	24.8	25.8	54	72	0.65	75.6

[a] To avoid shadowing problems, A401 was observed at (72+n72)m spacings for a full 12^h; at (36+n72)m for -3^h to $+3^h$ HA; and at (108+n72)m from -6^h to -3^h and from $+3^h$ to $+6^h$ HA.

TABLE II. — *Source list for Abell 401.*

SER. NUM. 14W	RIGHT ASCENSION (1950)	DECLINATION (1950)	FLUX DENSITY 610 MHz (mJy)	FLUX DENSITY 1415 MHz (mJy)	SPECTRAL INDEX	OPTICAL IDENTIFICATION Type	Δα″	Δδ″	NOTES
1	$02^h53^m34^s.0\pm0.1$	12°57′24″±5″	350±15	120±40	1.3±0.4	**G(17.6)	3	-2	22″ 94°, a
2	02 53 50.2±0.1	13 22 32 ±3	830±30	700±20	0.2±0.1	EF			PKS
3	02 53 58.9±0.1	13 17 16 ±7	87±7	35±5	1.1±0.2	*G(f)	-4	18	74″ 165°, b
4	02 54 27.0±0.1	13 13 14 ±3	73±5	42±5	0.7±0.2	**G(f)	-3	2	14″ 89°, c
5	02 54 30.1±0.2	13 23 43 ±18	<15	5.2±0.5	<1.2	PLOs			
6	02 54 41.0±0.1	12 46 09 ±4	140±40	32±6	(1.7±0.5)	G?(f)	-13	-6	d
7	02 54 51.9±0.1	13 01 31 ±12		5±2		EF			
8	02 54 52.9±0.1	12 48 56 ±5		41±5		EF			
9	02 55 01.1±0.1	13 13 29 ±3		6.6±0.7		PLOs			
10	02 55 07.8±0.2	13 13 59 ±10		3.4±0.4		EF			
11	02 55 25.2±0.1	13 20 29 ±4	59±4	24±3	1.1±0.2	EF			e
12	02 55 25.4±0.1	13 39 47 ±3	250±25	125±20	0.8±0.2	*G(16.3)†	1	-12	35″ 151°, f
13	02 55 30.4±0.2	13 44 10 ±7	39±4	23±5	0.6±0.3	EF			
14	02 55 30.9±0.1	13 16 31 ±5	<20	7.2±0.8	<1.2	**G(16.6)†	0	-2	
15	02 55 33.7±0.2	13 02 25 ±6	<15	4.1±0.4	<1.5	**PLO	0	1	20″ 85°
16	$02^h55^m46^s.9\pm0^s.1$	13°22′21″±5″	870±40	419±30	0.8±0.1	**G(16.2)†	-3	-1	g
17	02 55 53.1±0.1	13 02 08 ±8	25±4	11±2	1.0±0.3	**PLO	0	0	
18	02 56 09.3±0.2	12 58 03 ±12	<15	6.5±1.0	<1.0	EF			
19	02 56 17.9±0.1	13 30 20 ±3	165±30	53±6	1.3±0.3	EF			h
20	02 56 28.9±0.1	13 01 57 ±7	<20	10±2	<0.8	G(f)			
21	02 56 30.1±0.1	13 15 44 ±3	185±20	110±10	0.6±0.2	G(16.8)†	-12	11	38″ 59°, i
22	02 56 32.9±0.3	13 32 31 ±14	(28)	7±1		**PLO	1	-2	j
23	02 56 34.1±0.1	13 09 36 ±7	41±6	15±5	1.2±0.5	*G(f)	-4	5	
24S	02 56 52.5±0.2	13 42 50 ±10	1350±80	375±30	0.7±0.1				k
24N	02 56 53.6±0.1	13 43 18 ±20		355±30					

a) This galaxy could be a member of Abell 399.

b) The suggested identification appears to be the brightest member of a plate limit cluster. It lies 18″ southeast of the radio position (i.e. in the same position angle as the major axis of the radio source).

c) This galaxy appears to be in a plate limit cluster.

d) At 1 415 MHz the source is unresolved. At 610 MHz it is centered 30″ to the south, and is extended (60″ 73°). In addition to the faint galaxy listed, there are several PLOs close to the 1 415 MHz position.

e) At 1 415 MHz this source is polarized (9 %, $PA \sim 40°$). There is a faint galaxy at $\Delta\alpha = -31''$, $\Delta\delta = -6''$; and a PLO at $\Delta\alpha = 14''$, $\Delta\delta = 5''$.

f) A contour plot of this source is shown in figure 2.

g) This is the TRG, 4C13.17A (Fig. 1). The optical galaxy is No. 7 of Hintzen *et al.* (1977). Very little polarization was detected (1 415 MHz). Just to the west of the total intensity peak we find ~ 1 %, $PA \sim 10°$; which is close to the expected instrumental polarization. About halfway down the tail we find ~ 1.8 %, $PA \sim 115°$, but this is close to the noise level.

h) The 1 415 MHz flux density includes a contribution from low level emission which extends to the south and to the east. At 610 MHz, the southern extension is quite strong and almost reaches the position of the cD galaxy at the cluster center (see Fig. 4*a* and 4*b*).

i) 4C13.17B. The galaxy suggested as an identification is a companion of No. 4 of Hintzen *et al.* (1977). Their galaxy (16.0 *m*) lies at $\Delta\alpha = 0''$, $\Delta\delta = 26''$.

j) This source is included in figure 4*b*.

k) *24S* and *24N* are 2 components of 4C13.17C. Slingo (1974) gives a finding chart. The correct identification is probably a faint galaxy coincident with the radio centroid (see the discussion in the text and figure 3).

TABLE III. — *Source list fort Abell 1446.*

SER. NUM. 14W	RIGHT ASCENSION (1950)	DECLINATION (1950)	1415 MHz FLUX DENSITY (mJy)	OPTICAL IDENTIFICATION Type	Δα″	Δδ″	NOTES
25	$11^h57^m09^s.8\pm0^s.1$	57°59′43″±2″	80±12	EF			22″ 29°
26	11 57 14.3±0.1	58 37 02 ±1	1180±50	**PLO	1	0	Ohio, a
27N	11 58 31.3±0.6	57 56 41 ±6	60±10	EF			
27S	11 58 33.9±0.4	57 56 03 ±4	70±10	EF			
28	11 58 36.0±0.1	58 09 52 ±1	48±3	EF			
29	11 58 37 ±1.0	58 04 33 ±5	7±1	**S?(f)	-6	-2	
30	11 58 41.5±0.2	57 50 42 ±2	50±4	EF			
31S	11 58 47.4±0.5	58 23 51 ±4	95±15	EF			b
31N	11 58 50.7±0.5	58 24 11 ±5	140±15	EF			b
32	11 59 03.7±0.1	57 59 31 ±1	13±2	PLO			
33	11 59 31.1	58 18 49	826±40	**G(15.4)†	4	-1	c
34	11 59 52.4±0.2	58 04 59 ±3	8±1	PLOs			
35	12 00 14.1±0.2	58 02 34 ±1	19±3	**G(18.6)	-1	0	
36	12 01 05.6±0.3	58 53 49 ±2	160±50	EF			
37	12 01 22.8±0.1	58 36 27 ±1	49±5	PLO			

a) The optical position for which $\Delta\alpha$ and $\Delta\delta$ are listed refers to the center of an east-west double image.

b) The component separation is 33″ in PA = 52°. On the line joining the two components but closer to the stronger, lies a faint stellar object : $\alpha = 11^h58^m49^s.69$, $\delta = 58°24'02''.6$.

c) 4C58.23, α = 0.9. See contour diagrams, figures 5*a* and 5*b*. This dominating galaxy appears to have a double nucleus on the PSS blue print. We estimate the separation to be ~ 6″ in PA ~ 60°. At 4 995 MHz, the total flux density is 250 ± 20 mJy.

TABLE IV. — *Source list for Abell 1452.*

SER. NUM. 14W	RIGHT ASCENSION (1950)	DECLINATION (1950)	1415 MHz FLUX DENSITY (mJy)	OPTICAL IDENTIFICATION Type	Δα″	Δδ″	NOTES
38	$11^h58^m14^s.4\pm0^s.1$	51°54′31″±1″	22±4	EF			
39	11 58 36.2±0.1	52 21 56 ±1	45±10	PLO			
40	11 59 04.0±0.1	52 02 46 ±1	28±3	EF			a
41	11 59 51.1±0.1	51 47 55 ±1	61±5	EF			
42	11 59 58.0±0.1	51 42 15 ±1	42±4	EF			
43	12 00 27.0±0.2	52 06 31 ±2	11±2	**G(~18)	0	0	b
44W	12 00 26 ±1	51 56 58 ±3	185±20	EF			c
44E	12 00 35.1±0.1	51 56 53 ±4	440±40	G(15)†	9	-19	c
45	12 00 35.8±0.1	51 28 14 ±3	50±10	EF			
46	12 00 39.0±0.2	52 05 28 ±2	7.5±1.5	**G(16)	0	1	27″ 29°, d
47	12 00 44.0±0.1	51 48 55 ±1	18±2	EF			
48	12 01 18.8±0.1	52 04 40 ±2	17±3	EF			
49	12 01 32.7±0.1	51 42 08 ±1	37±6	**Gs?(f)	1	-	21″ 56°, e
50	12 01 46.0±0.1	52 19 00 ±1	940±40	EF			

a) There is a weak extension to the southwest at the noise level of the map. This would raise the total flux density to ~ 44 mJy.

b) This galaxy has a disc in PA ~ 45°. It lies about 23″ to the east of a brighter elliptical which is a background galaxy (No. 11 of Ulrich, 1978).

c) 4CP51.29a. See Miley and Harris (1977) for a 1 415 MHz contour diagram. The galaxy indicated is No. 1 of Ulrich (1978). The 4 995 MHz contour diagram is shown in figure 6. The flux density at 6 cm is 179 mJy for the eastern component and 51 mJy for the western component.

d) Ulrich (1978) gives z = 0.085, i.e. this is a background galaxy.

e) There are two objects ; the brighter lies 5″ south of the radio position and the fainter is 1″ north. Both appear to be members of a distant cluster.

TABLE V. — *Source list for Abell 1775.*

SER. NUM. 14W	RIGHT ASCENSION (1950)	DECLINATION (1950)	1415 MHz FLUX DENSITY (mJy)	OPTICAL IDENTIFICATION Type	Δα″	Δδ″	NOTES
51	$13^h38^m36^s.9\pm0^s.1$	26°44′20″±2″	24±2	**G(15.9)†	1	-1	
52	13 38 38.0±0.1	26 52 11 ±2	28±2	EF			
53	13 39 07.3±0.1	26 42 36 ±4	5.0±0.8	EF			
54	13 39 29.2±0.1	26 24 07 ±2	11±2	EF			
55	13 39 31.1±0.1	26 37 30 ±2	360±30	*G(15.2)†	3	9	4C, B2, a
56	13 39 37.6±0.1	26 14 31 ±3	49±4	EF			
57	13 39 37.8±0.1	26 20 58 ±2	38±3	EF			
58	13 39 44.4±0.1	26 18 59 ±2	17±5	EF			
59	13 39 49.2±0.1	26 45 48 ±3	9±2	**G(18.5)	0	0	
60	13 40 08.8±0.1	26 39 15 ±1	9±2	EF			
61	13 40 16.8±0.2	26 45 57 ±6	16±3	EF			b
62	13 40 25.8±0.1	26 02 24 ±2	240±40	EF			B2, Ohio,VRO, c
63	13 40 31.7±0.1	26 21 02 ±1	38±3	**PLO	-1	1	

a) The formal, 2-dimensional Gaussian fit to the high intensity peak gives 11″ in $PA = 62°$. The 500 kpc tail which curves off to the northeast is shown in the contour diagram of Miley and Harris (1977). Figure 7 shows our 4 995 MHz map. The integrated flux density is 80 mJy.

b) The source is probably extended, but the map intensity is not large enough to determine the size parameters accurately.

c) The search for optical candidates for this source was made with only the overlay technique.

TABLE VI. — Source list for Abell 2220.

SER. NUM. 14W	RIGHT ASCENSION (1950)	DECLINATION (1950)	1415 MHz FLUX DENSITY (mJy)	OPTICAL IDENTIFICATION Type	Δα″	Δδ″	NOTES
64	$16^h35^m55^s.7\pm0^s.1$	54°04′32″±1″	290±30	**G(19)	1	1	a
65	16 36 07.9±0.2	54 00 07 ±3	27±8	EF			b
66	16 37 00.3±0.1	54 00 44 ±2	6.2±0.6	EF			
67	16 37 12.5±0.1	53 39 29 ±1	49±3	EF			
68	16 37 16.2±0.1	54 00 24 ±1	29±2	EF			
69	16 37 25.2±0.1	53 57 37 ±1	58±5	EF			13″ 83°
70	16 37 31.2±0.1	53 56 38 ±1	11±3	EF			16″ 36°
71	16 37 34.0±0.1	53 40 48 ±1	32±2	EF			
72	16 37 38.4±0.1	53 40 23 ±1	10±3	EF			14″ 28°
73	16 38 04.0±0.1	53 34 38 ±1	14±2	**PLO	2	1	
74	16 38 24.1±0.2	53 52 11 ±2	630±30	G(14.9)†	-4	-19	4C,Ohio, c
75	16 38 32.4±0.1	54 03 33 ±1	245±15	*PLO	4	1	
76	16 39 12.0±0.1	54 02 35 ±1	33±3	**G(18.5)†	0	2	
77	16 39 22.8±0.2	54 01 51 ±2	14±2.	EF			
78	16 40 09.2±0.2	54 15 32 ±2	27±5	EF			
79	$16^h40^m52^s.3\pm0^s.1$	53°45′27″±1″	98±15	**G(16.3)	-1	1	d
80	16 41 21.7±0.3	54 14 40 ±3	39±6	EF			
81	16 42 01.2±0.1	53 51 07 ±1	116±15	EF			

a) This galaxy appears to be a member of a distant cluster.

b) The flux density includes a contribution from a weak extension to the east.

c) This galaxy is surrounded by a swarm of much fainter images. Our contour diagrams are shown in figures 8*a* and 8*b*. The WSRT flux density at 4 995 MHz is 210 ± 20 mJy and the spectral index is $\alpha = 0.8$ from 1 to 8 GHz.

d) The listed flux density includes a contribution from symmetrical wings which extend 1.5 to the east and to the west (see Fig. 9).

TABLE VII. — *Source list for Abell 2250.*

SER. NUM. 14W	RIGHT ASCENSION (1950)	DECLINATION (1950)	1415 MHz FLUX DENSITY (mJy)	OPTICAL IDENTIFICATION Type	Δα″	Δδ″	NOTES
82	$17^h07^m02^s.4\pm0^s.1$	39°59′49″±1″	60±15	*PLO	-1.4	-3.5	19″ 115°
83	17 07 14.5±0.1	39 30 50 ±1	45±5	EF			
84	17 07 47.8±0.1	39 35 18 ±1	11±2	EF			
85	17 07 50.3±0.1	40 13 30 ±3	45±10	EF			
86	17 08 33.9±0.2	39 44 05 ±4	3.7±1.0	PLOs			
87	17 08 57.8±0.1	40 10 21 ±2	65±5	EF			
88	17 09 10.6±0.1	39 40 26 ±2	5.0±0.5	EF			
89	17 09 15.5±0.2	39 42 59 ±2	21±3	**G(18.5)	2	2	39″x16″ 120°
90	17 09 17.8±0.2	39 45 11 ±2	635±30	*G(15)†	11	3	a
91	17 09 57.5±0.1	39 39 27 ±1	4.8±0.6	EF			
92	17 10 19.1±0.1	40 01 17 ±2	195±15	**PLO	0	0	B2
93	17 10 22.4±0.2	40 15 12 ±3	45±6	PLO			
94	17 10 49.3±0.1	40 11 08 ±2	128±12	EF			B2
95	17 10 53.5±0.1	39 38 14 ±2	20±3	EF			
96	17 10 56.8±0.1	39 39 25 ±1	9.5±1.5	EF			

a) 4CP, B2, Ohio : $\alpha = 1.07$. A contour diagram of this tailed radio galaxy at 1 415 MHz is given in Miley and Harris (1977). The integrated flux density at 4 995 MHz for that part of the source visible above the noise level (see Fig. 10) is 87 ± 8 mJy.

TABLE VIII. — *Source list for Abell 2255.*

SER. NUM. 14W	RIGHT ASCENSION (1950)	DECLINATION (1950)	FLUX DENSITY 610 MHz (mJy)	1415 MHz (mJy)	SPECTRAL INDEX	OPTICAL IDENTIFICATION Type	Δα″	Δδ″	NOTES
97	$17^h07^m13^s.2\pm0^s.6$	63°41′40″±6″	30±5			EF			
98	17 07 38.5±0.2	64 28 29 ±2	125±7			**PLO	-1	1	
99	17 07 43.1±0.1	64 08 10 ±1	180±20	85±8	0.9±0.2	EF			
100	17 07 44.0±0.4	64 16 07 ±3	34±6			*S(b)	-6	13	
101	17 07 53.1±0.2	63 55 03 ±2	85±6	70±15	0.2±0.3	EF			
102	17 08 28.0±0.2	63 41 59 ±2	67±6			EF			
103	17 09 25.2±0.2	64 37 11 ±3	44±7			EF			
104	17 09 44.1±0.4	63 46 10 ±4	37±5			EF			54″ 0°
105	17 10 17.5±0.4	64 33 38 ±3	68±8			EF			
106	17 11 05.4±0.2	64 20 31 ±1		4.4±0.5		**G(18)	-2	2	
107	17 11 20.2±0.4	64 04 23 ±3		4±1		EF			
108	17 11 27.2±0.4	63 48 00 ±2	33±4			EF			
109	17 11 28.1±0.1	63 59 35 ±1	51±4	33±3	0.5±0.2	EF			i
110	17 11 44.9±0.3	64 17 09 ±2		2.0±0.6		EF			
111	17 11 45.4±0.4	63 57 47 ±2		2.4±0.5		EF			
112	$17^h11^m50^s.3\pm0^s.2$	63°41′59″±2″	46±6	28±6	0.6±0.3	*PLO	-3	1	32″ 152° a
113	17 11 56.8±0.2	64 05 34 ±2		9±2		*G(15.9)†	0	-4	b
114	17 12 00.8±0.3	63 54 30 ±2		5±1		EF			
115	17 12 05.2±0.2	64 05 35 ±2	680±70	290±30	0.9±0.1	**G(16.1)†	9	13	c
116	17 12 41.3±0.2	64 12 56 ±2	22±4	9.6±0.6	1.0±0.2	EF			
117	17 12 42.8±0.2	64 06 35 ±2		2.1±0.2		*G(15.4)†	0	4	
118	17 12 46.0±0.2	64 10 23 ±1	145±30	66±10	0.9±0.2	*G(16.8)†	6	-1	d
119	17 12 55.8±0.2	63 51 06 ±2	220±30	140±20	0.5±0.3	*G(15.5)†	2	7	e
120	17 13 10.1±0.2	64 06 12 ±2	390±25	250±20	0.5±0.1	**G(15.2)†	1	2	23″ 28°, f
121	17 13 23.6±0.1	64 08 17 ±2	10±1.5	4.2±0.6	1.0±0.2	*G(16.0)†	-3	2	g
122	17 13 31.5±0.2	64 03 36 ±2		2.1±0.2		**G(16.4)†	-2	3	
123	17 13 47.8±0.1	64 19 25 ±1	19±2	13±3	0.5±0.3	*G(18.2)	0	5	
124	17 14 01.8±0.2	65 13 02 ±1	300±40			EF			
125	17 14 04.2±0.2	64 00 27 ±1	77±8	39±3	0.8±0.2	EF			
126	17 14 19.6±0.3	65 20 42 ±3	370±40			**G(17)	1	0	
127	$17^h14^m50^s.0\pm0.2$	64°06′09″±1″	180±30	85±10	0.9±0.3	**G(15.7)†	-1	1	h
128	17 15 15.7±1.2	64 42 58 ±17	180±30			**G(16)†	5	-8	73″ 0°, i
129	17 17 10.2±0.5	64 04 29 ±3	30±3			**G(f)	0	-2	
130	17 18 15.8±0.9	64 12 45 ±4	25±10			**PLO	-1	0	
131	17 19 41.5±0.3	64 07 32 ±2	1730±80			EF f			4C
132	17 19 52.7±0.4	64 20 09 ±4	74±8			**G(f)	5	-1	
133	17 20 26.1±0.2	64 13 12 ±2	330±15			EF			

a) The 610 MHz position is 5.6″ earlier and the size measurement gives 49″ in *PA* = 121°.

b) This galaxy is the westernmost source in figure 11*a*.

c) The original TRG, 4C64.20.1A (Fig. 11). The spectral index has been determined from our data together with those of Slingo (1974) and Haslam *et al.* (1978). The 610 MHz flux density from low level emission to the north and east of the TRG is about 200 mJy.

d) 4C64.20.1B, the *Goldfish* (see Fig. 11*a* 11*b*). Haslam *et al.* (1978) report a flux density of 35 mJy at 2 695 MHz.

e) The *Beaver*. There are several faint images around the galaxy. Figures 12 (*a* and *b*) show the contour diagrams. Haslam *et al.* (1978) report a flux density of 166 mJy at 2 695 MHz. This value is much larger than that expected from our 2-point spectrum.

f) 4C64.20.1C, The *Double* (see Fig. 11*a* and 11*b* and the data of Owen and Rudnick, 1977).

g) The listed identification is the closer of two galaxies in contact. These two galaxies are probably numbers 6 and 7 of Tarenghi and Scott (1976).

h) The *Embryo*. Contour diagrams are shown in figures 13*a* and 13*b*.

i) The *Bean*. A contour diagram at 610 MHz is shown in figure 14. The projected distance to the cluster center is 5.3 Mpc.

j) Haslam *et al.* (1978) report a flux density of 31 mJy at 2 695 MHz.

TABLE IX. — *Sources which are probably associated with A2255.*

SER. NUM. 14W	DESCRIPTIVE NAME	OPTICAL MAGNITUDE m_V	M_V	LARGEST SIZE (arcmin)	(kpc)	RADIAL VELOCITY[a] B (km s^{-1})	A & B (km s^{-1})	DISTANCE FROM CLUSTER CENTER (kpc)	LOG LUMINOSITY (10^7-10^{10}Hz) (ergs s^{-1})
113	-	15.9	-22.5	<0.2	<23	-	-	548	40.23[c]
115	TRG	16.1	-22.3	2.1	290	412	-256	530	41.86
117	-	15.4	-23.0	<0.2	<23	-	-	584	39.60[c]
118	Goldfish	15.8	-22.6	2.2	304	42	-626	547	41.16
119	Beaver	15.5	-22.9	3.0	400	-	-	2637	41.41
120	Double	15.2	-23.2	0.4	58	652	-16	966	41.67
121	-	16.0	-22.4	<0.2	<23	-604[b]	-1272[b]	1116	40.03
122	-	16.4	-22.0	<0.2	<23	-	-	1436	39.60[c]
127	Embryo	15.7	-22.7	4.8	664	-	-	2482	41.27
128	Bean	16.	-22.4	3.	400	-	-	5300	41.27[d]
-	Halo	-	-	10.	1400	-	-	-	41.87

[a] The column denoted "B" gives the difference between the velocity of the galaxy and the mean velocity of cluster B; entries in column A & B give the velocity difference relative to the mean for the one-cluster hypothesis.

[b] The other galaxy of the close pair gives values of 340 and -328 km s^{-1} for B and A & B, respectively.

[c] A value of $\alpha = 0.7$ has been assumed for those sources detected only at 1415 MHz.

[d] $\alpha = 0.9$ has been assumed for the "Bean".

TABLE X. — *Source list for Abell 2306.*

SER. NUM. 14W	RIGHT ASCENSION (1950)	DECLINATION (1950)	1415 MHz FLUX DENSITY (mJy)	OPTICAL IDENTIFICATION Type	$\Delta\alpha''$	$\Delta\delta''$	NOTES
134N	$18^h25^m52^s.7\pm0^s.2$	74°19′47″±1″	560	a			
134S	18 25 58.2±0.2	74 18 42 ±1	1260	a			
135	18 25 57.1±0.2	74 42 29 ±1	100±10	EF			17″ 114° b
136	18 26 23.8±0.4	74 41 58 ±2	300±40	**G(16.7)†	2	-9	c
137	18 26 34.3±0.4	74 43 10 ±2	50±10	**G(17.8)†	3	2	d
138	18 26 42.6±0.2	75 07 27 ±1	120±12	PLO			
139	18 27 01.4±0.7	75 06 59 ±2	40±20	EF			
140	18 28 04.6±0.2	74 31 39 ±1	48±5	**G(17.8)†	0	0	
141	18 28 04.9±0.2	74 41 10 ±1	15±2	EF			
142	18 28 31.4±0.2	74 44 12 ±1	36±6	**G(17.6)†	-1	0	
143	18 30 39.9±0.2	74 31 45 ±1	70±7	*PLO	3	1	
144	18 30 41.4±0.3	74 58 49 ±2	19±4	EF			
145	18 30 48.5±0.5	74 57 19 ±2	20±5	PLO			

a) 3C379.1 is identified with an 18.1 *m* galaxy with $z = 0.256$ (Smith *et al.*, 1976) at $\alpha = 18^h25^m55^s.90$, $\delta = 74°19'10''.2$. The total flux density from both radio components is 1.9 ± 0.1 Jy. See Högbom and Carlsson (1974) for a contour diagram.

b) *135* is included in figure 15. Rudnick and Owen (1977) resolve this source at 2 695 MHz. They show a close double with separation = 12″ at $PA = 124°$.

c) See figure 15.

d) The source appears extended in $PA = 20°$ (see Fig. 15). Because of this extension, we have also plotted the position of the center of a double galaxy ($m \sim 18$). There are many plate limit blue images surrounding this double galaxy. The center of the two images is at $\alpha = 18^h26^m34^s.46$, $\delta = 74°43'20''.4$.

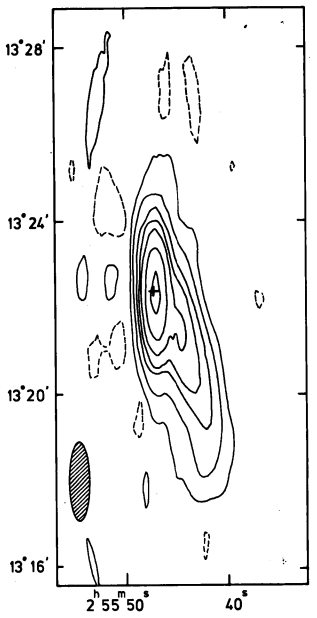

FIGURE 1. — The TRG in A401 at 1 415 MHz. The shaded ellipse shows the half-power dimensions of the synthesized beam. The cross indicates the position of the galaxy. The contour levels are — 0.5 % (dashed), 0.5, 2, 6, 10, 20, 40, and 80 % of the peak intensity which is 274 mJy/beam.

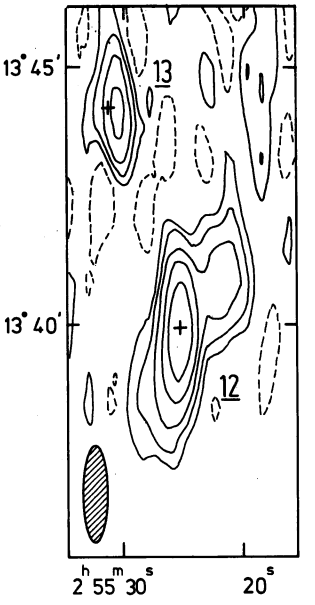

FIGURE 2. — Sources *12* and *13* in A401 at 1 415 MHz. The cross at the center of *12* indicates the galaxy position and the cross following the peak intensity of *13* locates the midpoint of a faint double image. Contour levels are ± 3.125, 6.25, 12.5, 25, and 50 % of the peak intensity which is 69.2 mJy/beam.

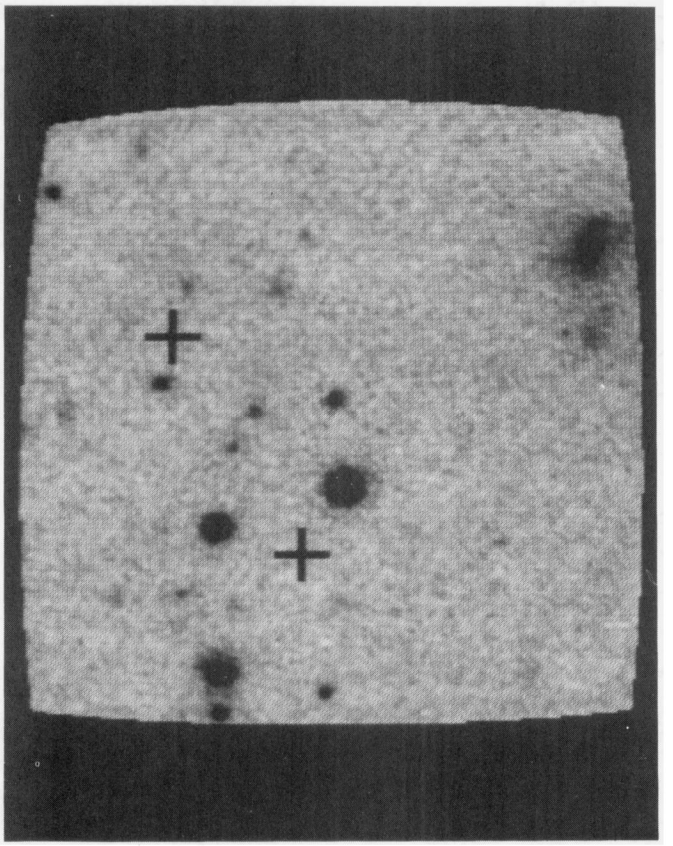

FIGURE 3. — A reproduction of an exposure on the field of 4C13.17C (*24*) from the KPNO 4 m telescope. North is up and east is on the left. The two crosses indicate the radio positions from table II. They are separated by 32 arcs. Slingo's (1974) two objects are the stellar images just above the lower cross and our suggested identification is the faint galaxy which is halfway between the radio lobes.

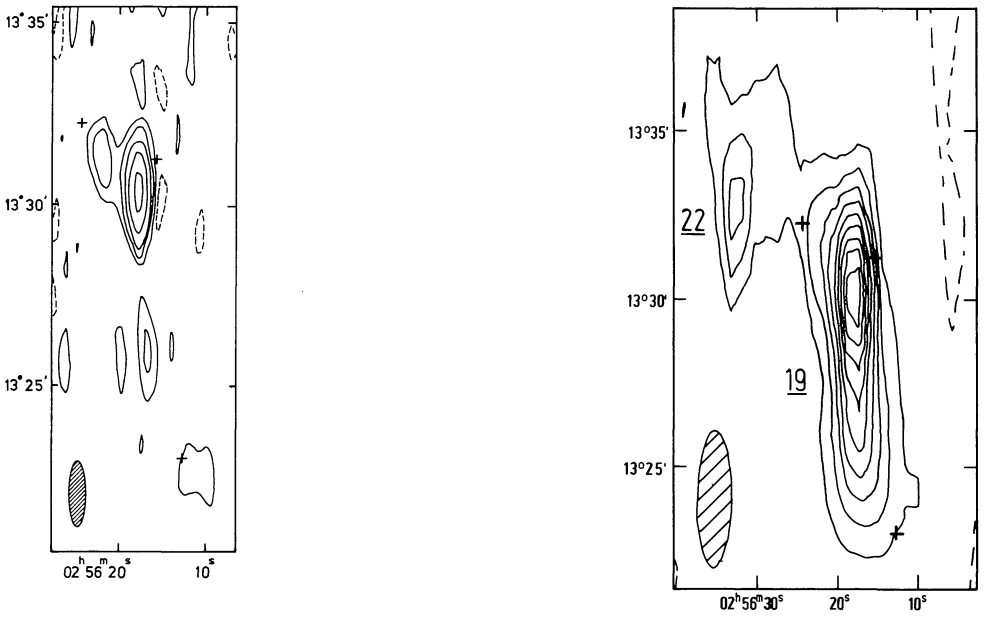

a) *b*)

FIGURE 4 (*a* and *b*). — Source *19* in A401. The northern two crosses indicate the positions of 16 *m* galaxies and the cross in the south locates the cD galaxy near the cluster center. *a*) The 1 415 MHz map with contour levels of ± 4, 8, 20, 40, and 80 % of the peak intensity which is 31.8 mJy/beam ; *b*) The 601 MHz map with contour levels of ± 10, 20, 30, 80, and 90 % of the peak intensity of 75 mJy/beam. Sources are identified by their numbers in table II.

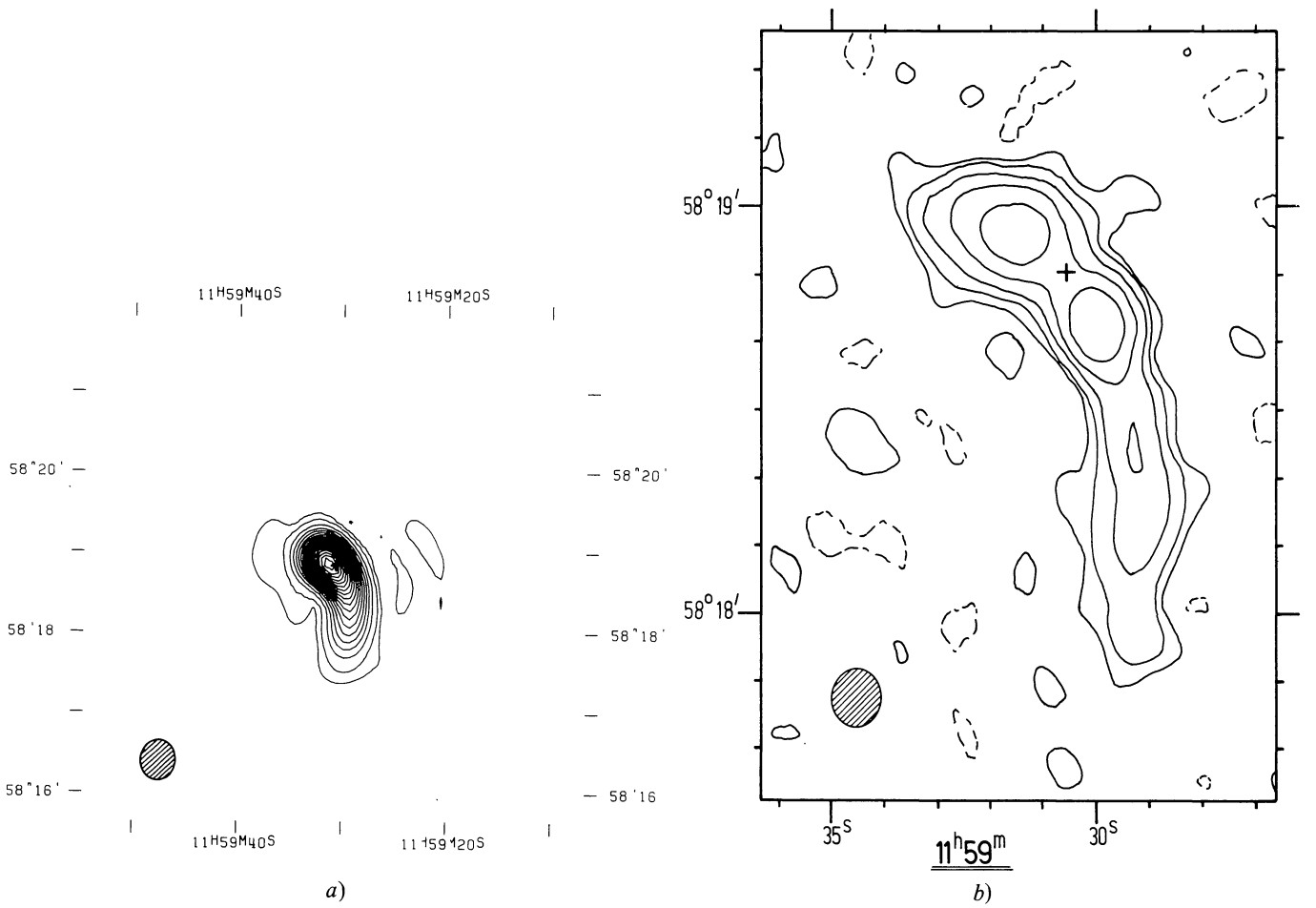

a) *b*)

FIGURE 5 (*a* and *b*). — Source *33* in A1446. *a*) The 1 415 MHz map with contour levels of 5 and then from 15 to 355 in steps of 20 mJy/beam ; *b*) The 4 995 MHz map with contour values of ± 3.125, 6.25, 12.5, 25, and 50 % of the peak intensity which is 54.9 mJy/beam.

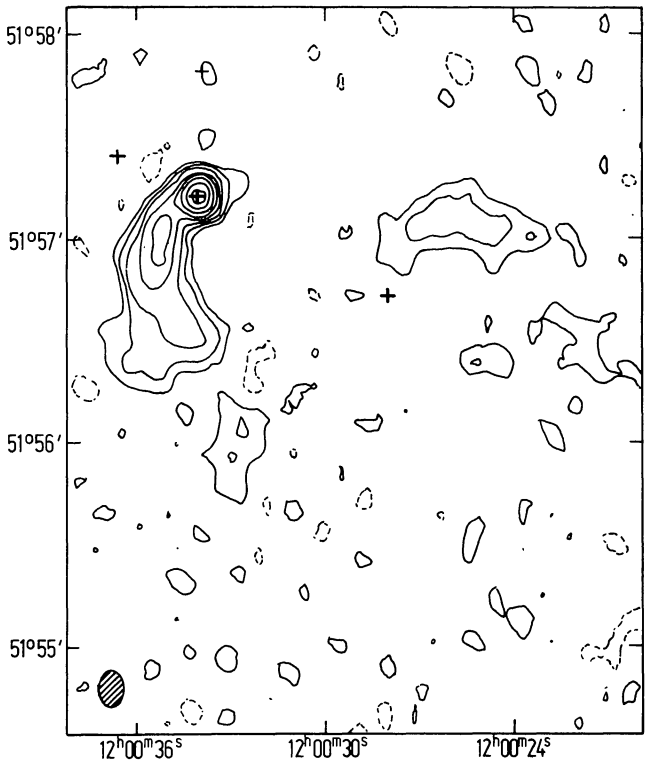

FIGURE 6. — Source *44* in A1452 at 4 995 MHz. Contour levels are ± 2.5, 5, 10, 20, 30, 40, 60, and 80 % of the peak intensity which is 46 mJy/beam.

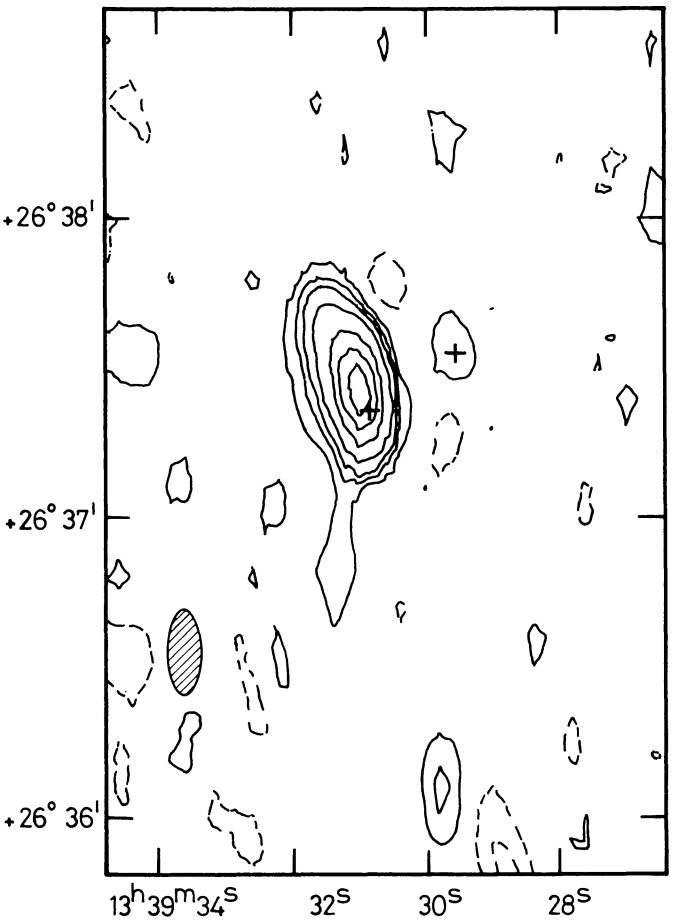

FIGURE 7. — Source *55* in A1775 at 4 995 MHz. Contour values are ± 4, 8, 12, 20, 40, 60, and 80 % of the peak intensity which is 48 mJy/beam.

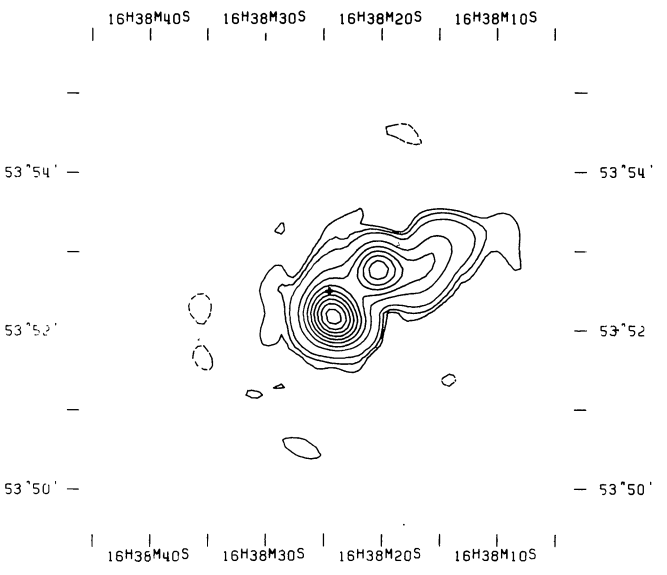

a)

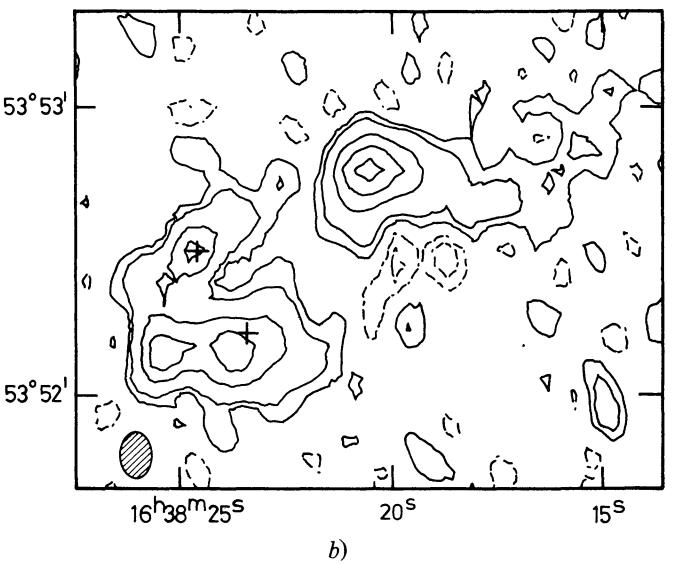

b)

FIGURE 8 (*a* and *b*). — Source *74* in A2220. *a*)The 1 415 MHz map with contour values of ± 2.5, 5, 10, 30, 50, 70, 90, 110, 130, 150, and 170 mJy/beam ; *b*) The 4 995 MHz map with contour values of ± 1.25, 2.5, 7.5, 12.5, and 17.5 mJy/beam. The lower cross indicates the position of an 18 *m* galaxy, one of the group of faint galaxies surrounding the giant elliptical (upper cross).

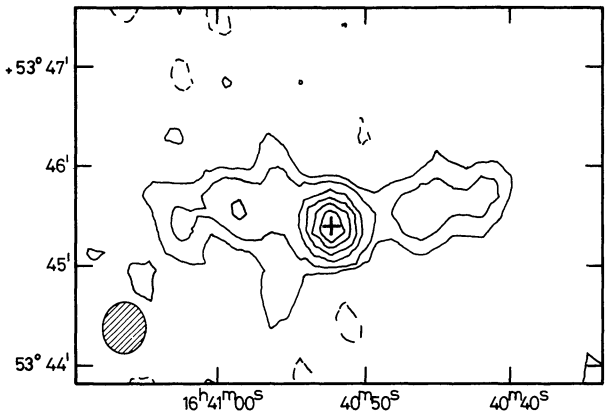

FIGURE 9. — A 1 415 MHz map of *79* in A2220. Contour values are ± 2.5, 5, 10, 15, 20, and 25 mJy/beam.

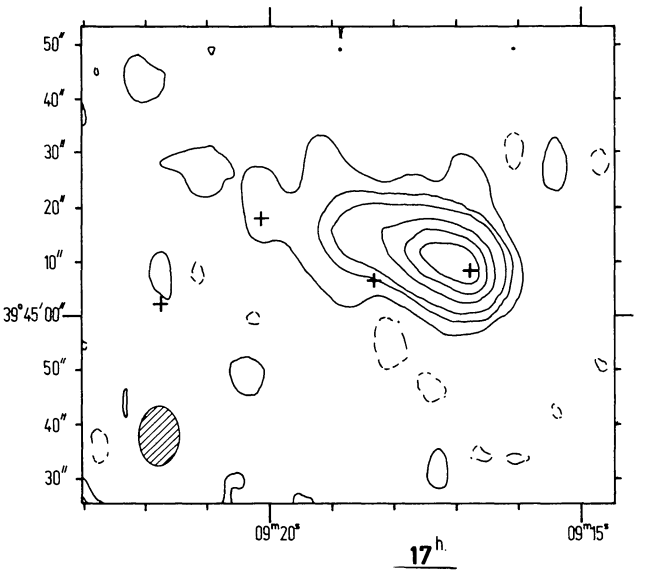

FIGURE 10. — The 4 995 MHz map of *90* in A2250. Contour values are ± 4, 12, 20, 40, 60, and 80 % of the peak intensity which is 24.1 mJy/beam.

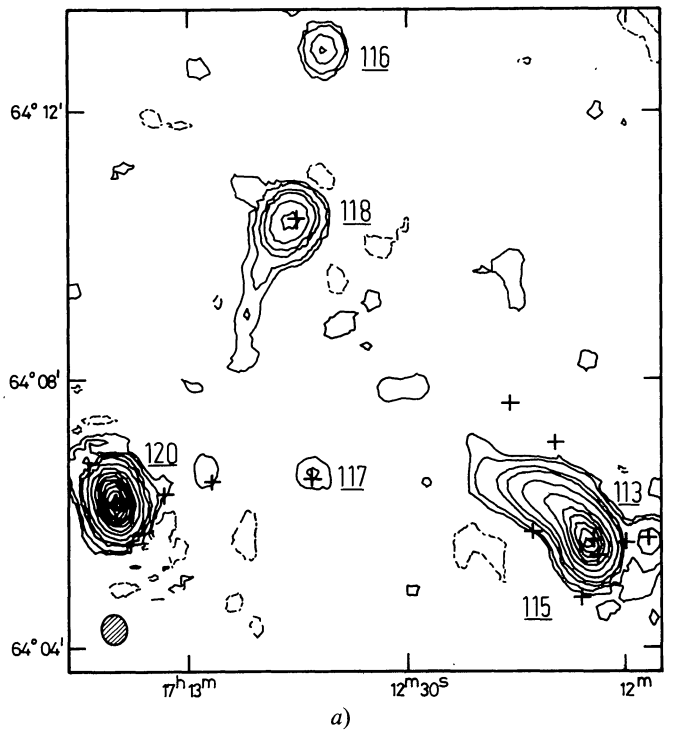

a)

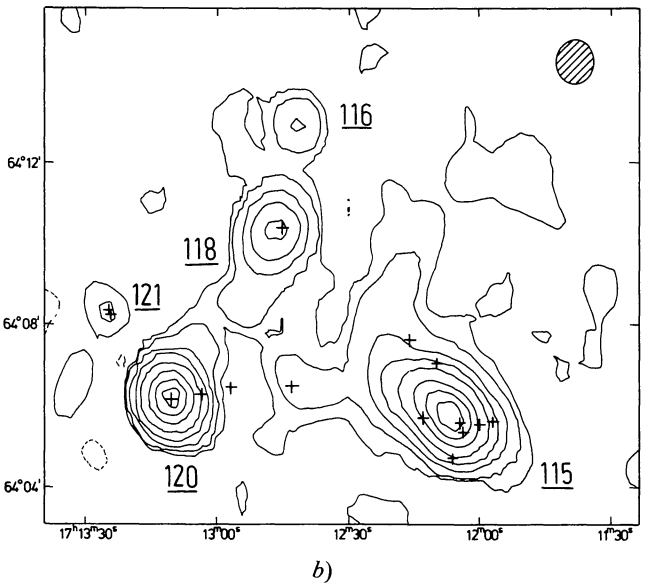

b)

FIGURE 11 (*a* and *b*). — The center region of A2255 : (*113, 115, 116, 117, 118,* and *120*). The crosses indicate the positions of bright galaxies. *a*) The 1 415 MHz map with contour values of ± 0.5, 1, 3, 5, 10, 20, 30, ... 80, and 90 % of the peak intensity which is 172 mJy/beam ; *b*) The 610 MHz map with contour values of ± 1, 2, 5, 10, 20, 40, 60, and 80 % of the peak intensity which is 375 mJy/beam.

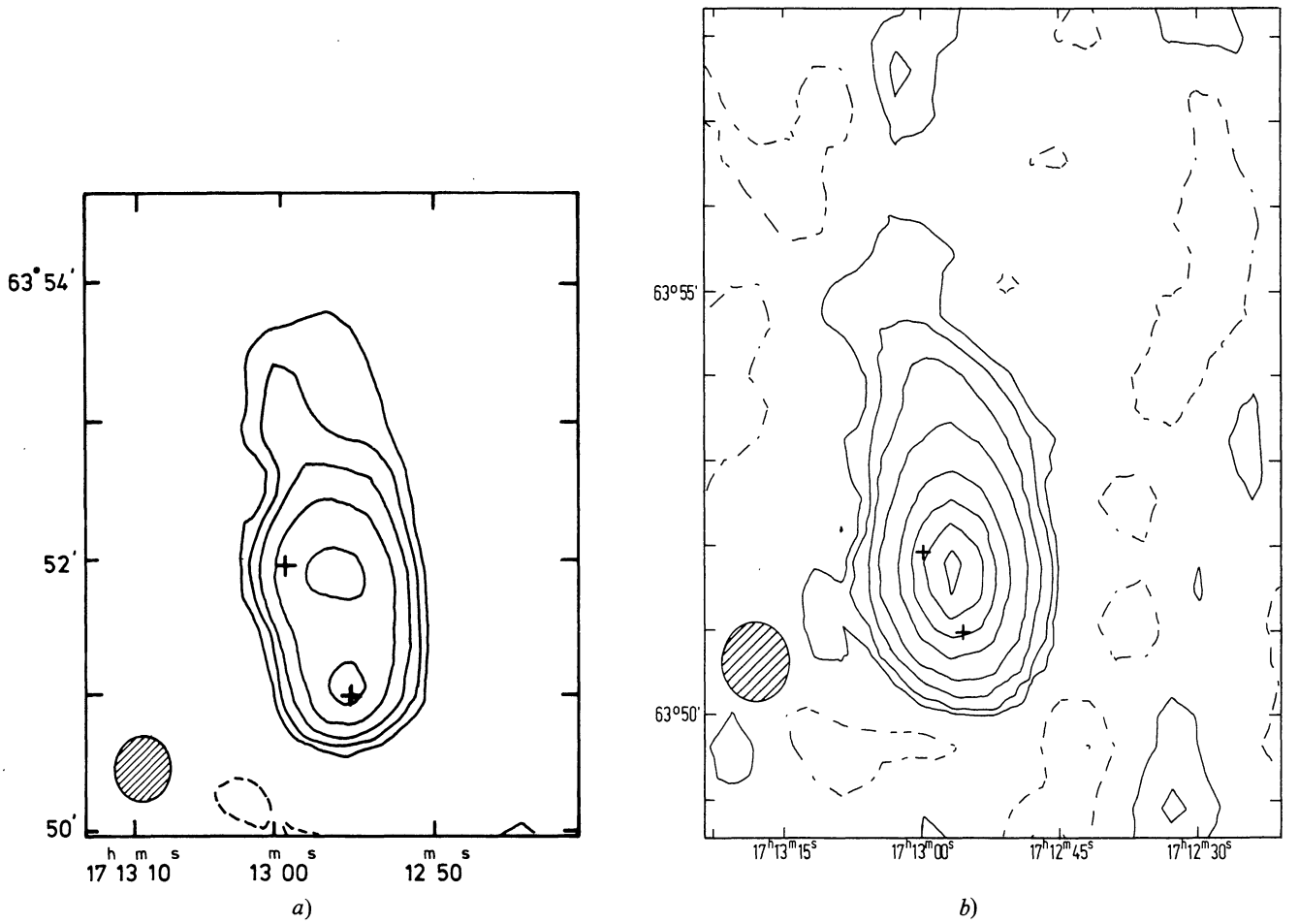

FIGURE 12 (*a* and *b*). — The *Beaver* (*119*) in A2255. *a*) The 1 415 MHz map with contour values of ± 5, 10, 20, 40, and 80 % of the peak intensity which is 24.6 mJy/beam ; *b*) The 610 MHz map with contour values of ± 2.5, 5, 10, 20, 40, 60, 80, and 100 mJy/beam.

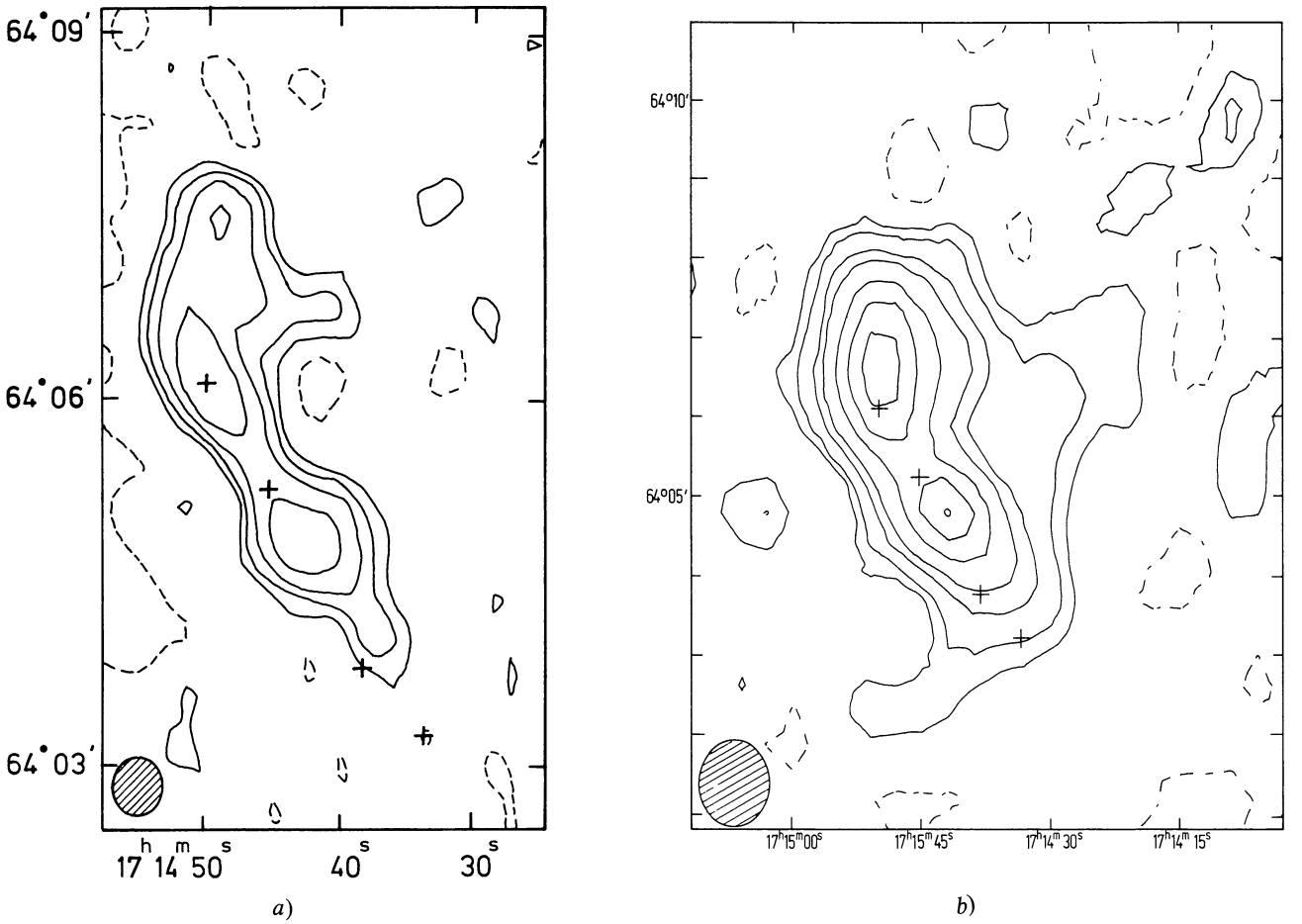

FIGURE 13 (*a* and *b*). — The *Embryo* (*127*) in A2255. *a*) The 1 415 MHz map with contour values of ± 6.25, 12.5, 25, and 50 % of the peak intensity which is 12.9 mJy/beam and coincides with the northernmost galaxy ; *b*) The 610 MHz map with contour values of ± 5, 10, 20, 30, 50, 70, and 90 % of the peak intensity which is 40 mJy/beam.

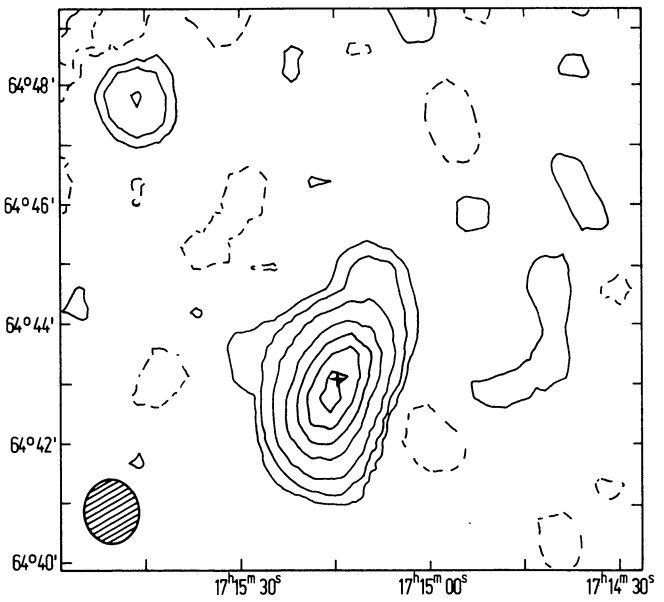

FIGURE 14. — A 610 MHz map of the *Bean* (*128*) in the A2255 field. Contour values are ± 3.8, 7.7, 15.4, 31, 46, 62, and 77 mJy/beam.

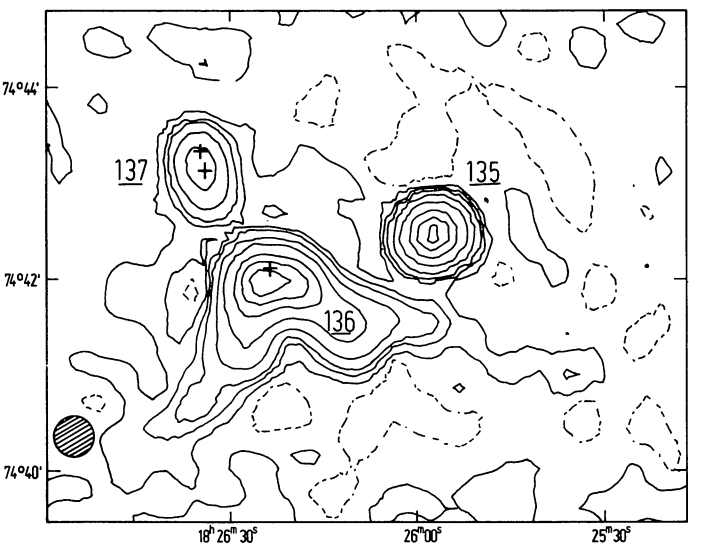

FIGURE 15. — The 1 415 MHz map of the center of A2306. Contour values are ± 1, 3, 5, 10, 20, 40, 60, and 80 % of the peak intensity which is 85 mJy/beam.